Journal of Theoretical Medicine, June 2003 Vol. 5 (2), pp. 93–110

Taylor & Francis
healthsciences

Modeling the Cytokine Network *In Vitro* and *In Vivo*

JOHANNES MÜLLER[a,*] and THORSTEN TJARDES[b]

[a]*Technical University Munich, Centre for Mathematical Sciences, Bolzmannstr. 3, D-85748 Garching / Munich, Germany;* [b]*University of Cologne, Biochemical and Experimental Division, 2nd Department for Surgery, University of Cologne, Ostmerheimerstr. 200, D-51109 Cologne, Germany*

(Received 22 July 2003; In final form 11 December 2003)

The present paper consist of two parts: in the first part an experiment investigating the endothelial cell/interleukin 1 system is analyzed by means of a model. The most interesting outcome is a bistability of the system: a small challenge will not lead to a reaction, while a challenge slightly above a certain threshold leads to a complete activation of the endothelial cells. This finding is used in the second part of the paper, where a caricature model of the innate immune response (the part of the immune system that is not based on acquired immunity) is described and analyzed. In this analysis, especially, the possible patterns of the dynamics in the absence of a challenge have been targeted. We find a variety of behaviors possible for the resulting planar system. For certain parameter values, a small challenge is ignored, while a challenge above a certain threshold leads to a massive strike of the immune system that comes eventually to rest again. Also bistability, periodic behavior or an unstable resting state can be found. It is heuristically possible to link most of these dynamical patterns with natural or pathological situations that can be found in clinical pictures.

Keywords: Immune system; Inflammation; Bifurcation analysis; Takens–Bogdanov bifurcation

INTRODUCTION

In the last two decades, immunology has attracted more and more attention. A lot of contributions to this field, not only from the experimental sciences but also from the theoretical point of view revealed many aspects of the immune system. Classical models for HIV (Novak and May, 2000), release of Histamine (Perelson, 1987) or the description of receptor-antibody binding (Lauffenburger, 1993) are well known in the community.

In this paper, we aim especially at a description of the inflammatory response in the early phase. We do not investigate the adaptive but only the innate part of the immune system. There is strong evidence that this part of the immune system plays a crucial role in the deterioration of the health status of polytraumatized patients (simultaneous injury of multiple regions of the body or organ systems with one of those injuries or the combination of injuries being life threatening, Tscherne 1978). The physiologic reaction of the organism is an inflammatory response, especially with local proinflammatory signals, resulting in an over-stimulation of the unspecific immune system. Consequently, the inflammatory reaction cannot be contained at the site of the primary insult which leads to a generalized inflammatory result with impairment of organ function and tissue destruction even at sites distant from the insult (systemic inflammatory response syndrome (SIRS)). This process leads to multiple organ failure (MOF) and may ultimately result in the death of the patient. Based on these theories it should be possible to predict behavioral patters. However, there have been no advances so far to arrive at a deeper understanding of the dynamics underlying this inflammatory response.

Many parts of this system are experimentally well investigated (see e.g. Baue *et al.*, 2000). The most intriguing part is the communication between different cell types (that are partially distributed all over the body) by means of chemical additives, so-called mediators. A complex network of communicating cells and regulatory pathways evolves the network of cytokines. Until now, this system did not attract too much attention from the modeling community. Laufenburger described how lymphocytes are invading tissue attacked by a pathogen (Lauffenburger and Kennedy, 1981; Alt and Lauffenburger, 1985). Seymour and Henderson (2001) recently described a model of the lymphocyte/interleukin 1 system, and found a variety of possible behaviors. Their model can exhibit even chaotic behavior for certain parameter values. An individual based model targeting the effect of sterile or infected injuries is described in

*Corresponding author. E-mail: johannes.mueller@gsf.de

ISSN 1027-3662 print/ISSN 1607-8578 online © 2003 Taylor & Francis Ltd
DOI: 10.1080/1027336042000208642

An (2001). Simulations of this model show, that the system either recovers or fails to recover, depending on the seriousness of the initial injury.

This paper consists of two parts that—in a certain sense—present two extreme approaches. The first part concentrates on an *in vitro* experiment with interleukin 1 and endothelial cells. These are one single node and respective edge in the cytokinic network. The behavior of this specific cell type in connection with this specific mediator will be analyzed in detail. This experiment is interesting, first since endothelial cells are located at the interface between tissue and blood. They amplify signals and, in this way, control a large part of the proinflammatory signaling cascade. Second, challenged endothelial cells produce interleukin 1. Thus it is possible to study one of the major positive feedback loops of the proinflammatory reaction in an *in vitro* experiment.

The other extreme is a caricature of the inflammatory system, that lumps the complex regulatory network into three components: pathogenic challenge, direct inflammatory reaction and control of the inflammatory reaction. Though oversimplified, this model incorporates the leading medical theory about the overall structure of the innate immune system. Seriously taking these theories, it is possible to predict behavioral patterns. Comparison with experimental and clinical observations reveals whether these basic assumptions are appropriate or too simple to meet reality. Beyond the phenomenological level this model explores the concept that has been the theoretical foundation of all attempts to treat the MOF syndrome, i.e. in case of an adequate stimulus the organism mounts a proinflammatory response, followed by an anti-inflammatory response. According to this concept a massive anti-inflammatory therapy (e.g. antibodies against proinflammatory mediators) was considered as an effective approach. Thus the model presented here will provide information whether the theoretical concept of past therapeutic approaches is valid or whether more sophisticated interventions have to be developed.

THE KEY PLAYERS

Cell Lines

Among the many different cell types of the organism, endothelial cells and leucocytes are of special importance in the early phase of an inflammatory insult. Forming the barrier between tissue and blood, endothelial cells are able to recruit white blood cells to the site of an inflammatory focus by expressing a set of special receptors on their cell surface (Shrotri *et al.*, 2000). Beyond that, endothelial cells are able to release a large number of cytokines that amplify the inflammatory response. While under physiologic conditions the inflammatory reaction is locally contained as endothelial cells do excrete antiinflammatory cytokines as well there are obviously conditions under which a generalized activation of endothelial cells occurs. The second cell type involved in the initial phase of an inflammatory reaction is white blood cells. In the inactivated state these cells circulate with the blood stream. If they pass activated endothelial cells their pace is slowed down by receptor interactions. Once the white blood cells are firmly attached to the endothelial cells leucocytes start to translocate through the endothelial barrier and secrete cytotoxic substances (oxygen radicals, proteolytic enzymes). The genuine purpose of this mechanism is the destruction of invading pathogens. As these cytotoxic substances act unspecifically, other cells, including endothelial cells, are damaged as well. This process finally results in organ damage and failure of organ function. While the physiologic purpose of this reaction is the local elimination of pathogens, which could be microorganisms as well as dead cells, the injury itself may serve as a sufficient stimulus for the pathologic activation of the proinflammatory pathway in the trauma patient.

Mediators

The interactions among endothelial cells and leucocytes are mediated by various substances. The cytokines are among the most powerful mediators that occur in the organism. Cytokines are not stored as preformed molecules but rather are produced on demand by active gene transcription and translation by injured or stimulated cells. Once released into the circulation, cytokines function predominantly via paracrine and autocrine mechanisms, i.e. primarily locally. In the case of a massive secretion of cytokines a spill over effect occurs resulting in cytokine effects even at remote sites of the organism. These mediators regulate the production and activity of other cytokines as well, resulting in an augmented (proinflammatory) and/or attenuated (anti-inflammatory) response. Challenging substances are e.g. LPS (toxic component of the bacterial cell membrane), via a complex with soluble LPS receptors (Pugin *et al.*, 1993), TNF (Dixit *et al.*, 1990) and IL-1 (Warner *et al.*, 1987) to name but a few. They all activate ECs. In consequence, ECs start to produce and release IL-1 (Warner *et al.*, 1987), prostaglandin PGE_2 (Warner *et al.*, 1987), IL-6 (Sironi *et al.*, 1989) and IL-8 (Pugin *et al.*, 1993) among other mediators. Prostaglandin PGE_2, in turn, decreases the production of mediators by activated EC (Dixit *et al.*, 1990). IL-6 seems not to have a direct effect on ECs (Sironi *et al.*, 1989). Hence, we have a positive feedback loop (IL-1 activates ECs, which in turn produces IL-1) and a negative feedback (activated ECs produce prostaglandin PGE_2, which downregulates ECs). Since the experiment we consider for the present model concentrates on the first 24 h, the downregulation by PGE_2 seems not to play a central role. In our model, we neglect this negative feedback (Table I).

TABLE I Selection of the most important cytokines involved in the early phase of the inflammatory response at the endothelial barrier

Cytokine	Source	Action
Tumor-Necrosis-Factor (TNF)	Endothelial cells, neutrophils	Promotes expression of adhesion molecules, coagulation activation, increases PGE_2 release
Interleukin-1 (IL-1)	Endothelial cells, neutrophils	Promotes expression of adhesion molecules, coagulation activation, increases PGE_2 release
Interleukin-6 (IL-6)	Endothelial cells, neutrophils	Attenuation of IL-1 and TNF activity, induction of neutrophil activation
Interleukin-8 (IL-8)	Endothelial cells	Chemotaxis for neutrophils

IL-1 and TNF are highly redundant concerning their principal effects but they operate on different time scales. The physiologic action of the mediators listed here are only a selection of the most important effects in the early inflammatory phase. For each of the mediators many additional functions have been documented.

IN VITRO MODEL

The Experiment

A large number of *in vitro* and *in vivo* experiments have been performed in order to investigate the effect of challenges on endothelial cells (Fig. 1).

The positive feedback loop is of special interest here. Is this feedback loop able to destabilize the inactive state of the EC's, or is the inactive state stable? If the inactive state is stable, is there nevertheless a stable active state? We will describe an experiment performed by an Italian group (Sironi *et al.*, 1989) in the next paragraph, model the situation in section "The Model", and analyze the data in section "Data Analysis".

In an experiment, an EC cell line is challenged with IL-1. The resulting IL-6 production is measured. The mediator IL-6 has the advantage of not being involved in the positive or negative feedback, and hence provides a substitute variable for the state of the ECs. If one investigates IL-1 directly, then the main difficulty is to distinguish between newly produced IL-1 and the IL-1 used to challenge the cells (Dixit *et al.*, 1990). Two experiments are of special interest for the present work: first, ECs have been challenged with different amounts of IL-1. The density of IL-6 has been measured after 24 h. Second, the time series of IL-6 density, given a certain challenge, has been measured. The combination of the two experiments allows one to describe the dynamics as well as the dose dependency of the activation. The data are shown in Fig. 2.

The Model

IL-1 attaches to receptors that trigger a signaling cascade. At the end of this cascade the endothelial cell starts to produce certain mediators and enhances the production of others. Especially, IL-1 is produced and the production of IL-6 is enhanced.

Of special interest is the mechanism that initiates the signaling cascade. Generally speaking these processes are enzymatically driven, i.e. even a small amount of IL-1 is able to produce a reasonable effect—a stimulation of about ten receptors may lead to the activation of a cell (Dinarello, 1996). Lauffenburger (1993) proposes a simple model covering the basic features: the dependence of the activation rate $r(A)$ on the density of the activating A substance is given by a Hill function,

$$r(A) = \frac{aA^m}{1 + bA^m}$$

where a, b and m are positive constants.

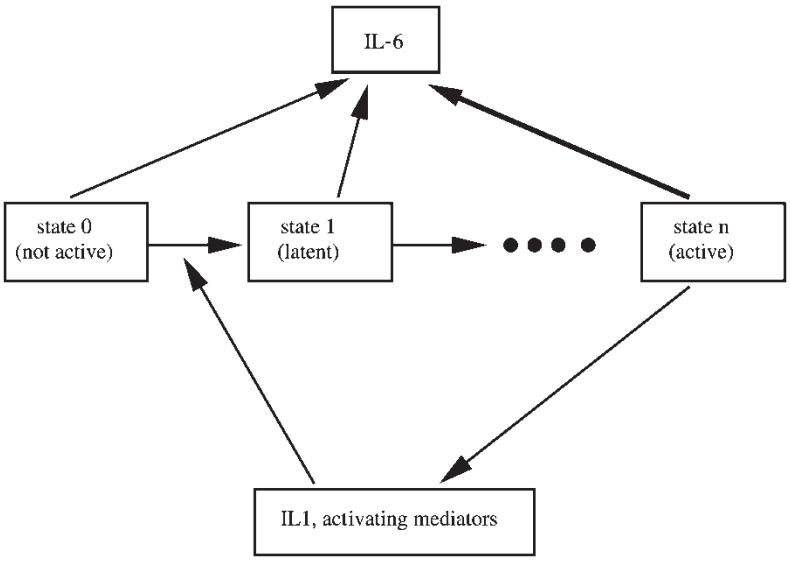

FIGURE 1 Structure of the model.

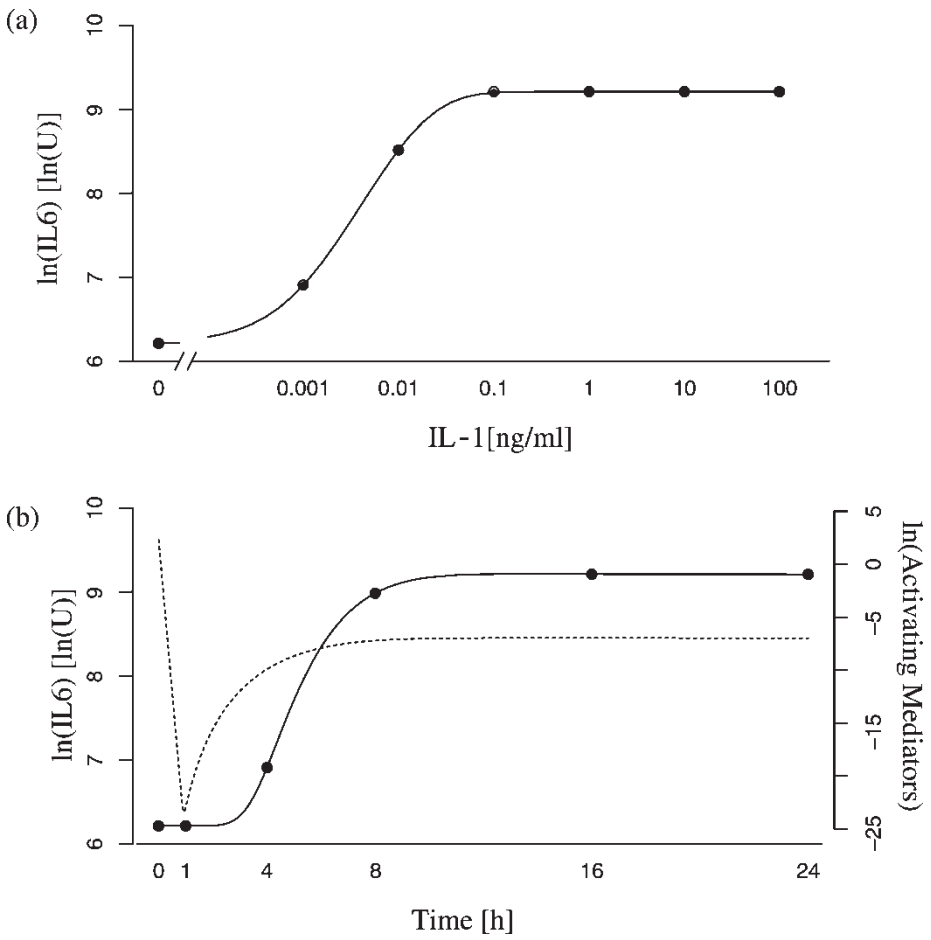

FIGURE 2 (a) Logarithm of IL-6 concentration (in 1000 U/ml) after 24 h for a given dose of IL-1 (units of the x-axis are ng/ml in a logarithmic scale). Data points and best prediction (solid line) are shown. Note that the leftmost data point belongs to a dose of zero ng/ml IL-1. (b) Dynamics of IL-6 and activating mediators (e.g. IL-1) over time. Predicted IL-6 density is shown as a solid line, the data are represented by points and the predicted density of IL-1 is shown as a dashed line. The initial dose of IL-1 is 10 ng/ml. Note that the steep increase of activating mediators at the time point of one hour is only a result of the logarithmic scale of the y-axis.

The cells are assumed to be in one of $n+1$ states: in state zero a cell is not activated. States 1 to $n-1$ are subsequentially transversed on the way to the activated state n. The signaling cascade consists of n different steps. The transition rate from state zero to one is $r(A)$. We do not have direct information about the time scales of states i, $i = 1, \ldots, n$. We assume that the transition rate δ is approximately the same for every state $1, \ldots, n-1$. Hence, the number of these states and the transition rate rather provide information about the magnitude and the variance of the time delay between the initiation of activation and the start of the release of mediators rather than the exact number of states between these two events. However, the number n may nevertheless give a crude hint in which magnitude the number of steps may range. From the activated state n the cells may relax and return to the inactive state. The biological mechanism that leads to this relaxation is the reduction of the receptor density on the cell surface with a desensibilization as consequence. Since we are interested especially in the first hour of the system, we do not take into account this effect but model the relaxation with a constant rate γ_x. The state variables $x_0, \ldots, x_n$ give information about the excitation of the system. There are two ways to interpret these variables: either $x_i(t)$ is the probability of finding a randomly chosen EC in state i or all cells behave alike, and are able to be gradually excited. Then, the vector $(x_0(t), \ldots, x_n(t))$ represents the degree of activation of the cells.

We consider two (classes of) mediators: $A(t)$ denotes the lumped quantity of all activating mediators in the system. Since we only have information about IL-1 at time zero, we normalize the influence of all activating mediators in units of ng/ml IL-1. We assume that all the relevant activating mediators are degraded with approximately the same rate γ_A. The activating mediators are only produced in state n with rate α. The second mediator is IL-6 with density IL(t). This mediator is released with rate r_0 if the cells are not activated (states $0, \ldots, n-1$), and with rate $r_0 + \beta$ if the cells are in state n. We also assume that the half-life of IL-6 is about the same as IL-1. We do have information about the amount of IL-6 and will use this information in order to fit the parameters.

TABLE II Estimation of the different parameters

Variable	0.025 Quart.	Median	0.975 Quart.	Max. Likeli
σ	0.0031	0.0051	0.0092	0.0033
m	1.05	1.059	1.07	1.058
a	471	533	598	531
b	0.0049	0.0050	0.0051	0.005
γ_x	0.002	0.00205	0.00211	0.00209
δ	7.50	7.53	7.56	7.53
η	14	14	14	14
γ_A	21.93	27.51	29.33	28.60
α	0.015	0.027	0.032	0.028
β	9671	9707	9744	9707
r_0	497	500	505	500
Log-Likeli	132034	1497189	159780	162273

The 95% confidence interval is shown, together with the parameter set that has the highest likelihood.

The model equations read

$$\begin{aligned}
&\dot{x}_0(t) = -r(A)x_0(t) + \gamma_x x_n(t), && x_0(0) = 1,\\
&\dot{x}_1(t) = r(A)x_0(t) - \delta x_1(t), && x_1(0) = 0,\\
&\dot{x}_i(t) = \delta(x_{i-1}(t) - x_i(t)), && x_i(0) = 0,\\
& && i = 2,\ldots,n-1,\\
&\dot{x}_n(t) = \delta x_{n-1}(t) - \gamma_x x_n(t), && x_n(0) = 0,\\
&\dot{A}(t) = -\gamma_A A(t) + \alpha x_n(t), && A(0) = A_0,\\
&\dot{\mathrm{IL}}_6(t) = -\gamma_A \mathrm{IL}_6(t) + r_0 + \beta x_n(t), && \mathrm{IL}_6(0) = \mathrm{IL}_{60},
\end{aligned} \tag{1}$$

where A_0 and IL_{60} denote the initial amount of activating mediators (i.e. IL-1) and IL-6, respectively (Table II).

Analysis of the Model

First of all, it is not necessary to consider the model for the whole parameter space. We are interested in the case of certain time scales. Especially, IL-1 is degraded very fast (time scale: minutes) in comparison with the activation of endothelial cells (time scales: hours), i.e. γ_A is high. Consequently, the amount of IL-1 present in the system will be (after a thin initial time layer) rather small. Even a small amount of IL-1 has an influence on the dynamics of the system, so the rate $r(A)$ has to be very sensitive.

Furthermore, the "recovery" rate γ_x of endothelial cells is small; endothelial cells will need a relatively long time (days) to relax. We exploit these three time scales (minutes, hours and days). This view is supported by the parameter fit shown in the next paragraph.

The next proposition exploits the time scale of IL-1 degradation and the resulting level of IL-1, respectively the sensitivity of rate $r(.)$ on IL-1 (for the proof see Appendix A).

PROPOSITION 3.1 Let $\hat{\gamma}_A = \epsilon\gamma_A$, $A = \epsilon B$ and $r(A) = \hat{r}(A/\epsilon)$. For $\epsilon \to 0$, this yields a singular perturbed system. The corresponding slow system reads

$$\begin{aligned}
&\dot{x}_0(t) = -\hat{r}(B)\,x_0(t) + \gamma_x x_n(t),\\
&\dot{x}_1(t) = \hat{r}(B)\,x_0(t) - \delta x_1(t),\\
&\dot{x}_i(t) = \delta(x_{i-1}(t) - x_i(t)),\\
&\dot{x}_n(t) = \delta x_{n-1}(t) - \gamma_x x_n(t),\\
&B(t) = \frac{\alpha}{\hat{\gamma}_A}\, x_n(t).
\end{aligned} \tag{2}$$

Now we exploit the slow time scale of the relaxation of endothelial cells. We find the following result (proof in Appendix A)

THEOREM 3.2:

(1) There is always a trivial stationary point $x_0 = 1$, $x_i = 0$ for $i = 1\ldots n$.
(2) If $r'(0) = 0$, then the trivial stationary point is always linearly stable.
(3) If $r'(0) > 0$, then the trivial stationary state is linearly stable provided that γ_x is large enough, and unstable if γ_x is sufficiently small.
(4) If γ_x is large enough, there is only one stationary state. If γ_x is small enough, there is at least one more positive stationary state. We order the stationary states by their nth component. Let $x^* = (x_0^*, \ldots, x_n^*)^T$ be the stationary state that has the largest nth component of all stationary states. Then $x_n^* \to 1$ if $\gamma_x \to 0$.
(5) x^* is linearly stable if γ_x is sufficiently small.

Remark There is a big difference between the case $m \le 1$ and $m > 1$. Since γ_x is small, the state with only relaxed endothelial cells is not stable for $m \le 1$. A perturbation, arbitrarily small, is able to activate the system. This is biologically not reasonable. If this situation occurs in the data analysis, this is a hint that the model has to take into account further effects, e.g. the effect of PGE_2.

If $m > 1$, then there will be (at least) two locally stable equilibria: the non-activated, resting state and the active state. A small amount of initial IL-1 has no effect. The system will return to the stable equilibrium. Only if the challenge crosses a certain threshold, the system reacts. Heuristically (though not proven) the system will run into the locally stable active state x^*. We observe this behavior in the experiment as well as in simulations. The threshold is determined especially by m (the closer m is to one, the smaller the threshold) and γ_x (the smaller γ_x the smaller the threshold).

Data Analysis

The model yields the expected value of IL-6 at a given point of time and a given amount of challenging IL-1. In order to use statistics, we define a variance structure. We assume that

$$\text{data point} = \text{value predicted by the ode} + e$$

where the error variables e are—for each data point—distributed according to a normal distribution with a variance proportional to the expected value,

$$e \sim N(0, \text{ value predicted by the ode} \times \sigma^2).$$

We do not assume a correlation between the error related to different data points. In order to obtain an idea about the magnitude and the confidence intervals for the estimates of the parameters, we use a Bayesian approach. We sample a Monte Carlo Markov Chain Model by a Metropolis Hastings algorithm (see Gilks *et al.*, 1998). However, since we do not use a sophisticated approach, the confidence intervals are rather descriptive and give a feeling for the precision of the estimates. One should not take this set of parameters too seriously. However, the model fits the data quite well (see Fig. 2), and some conclusions can be drawn.

(a) The time scale of half-life of IL-1 (about 3 min) agrees with *in vivo* findings (Dinarello *et al.*, 1987) (about 5 min). This information has been encoded only very indirectly via the data and the model structure. The relatively good estimation is remarkable.
(b) The same is the case for the relaxation rate: according to this rate an EC would relax in 20 days. Although this is ten times more than the two days observed in experiments, one has to take into account that the data and the model aim especially on the onset of activation, i.e. this estimation is sufficiently close.
(c) The positive feedback loop clearly plays a role, even in this relatively small experimental system. That is, the confidence interval of α is bounded away from zero.
(d) The most interesting parameter is without doubt the parameter m. If m is below one, the resting state is not stable, while it is stable if m is above one. We find that m is above, but very close to one. This indicates that the resting state is stable, but a relatively small dose of IL-1 is able to activate the system. ECs are easily stimulated. This finding is in agreement with the biological hypothesis about the function of ECs as a kind of guard at the boundary between the signaling pathways, the vessels and the tissue. This result is in agreement with other experimental data, where the mRNA level of IL-1β has only been sustained over 24 h if IL-1 itself has been a stimulus. There are other stimulants that initiate an increased mRNA level which starts to decrease again after 4 h (Dinarello, 1996).

All in all we find that resting endothelial cells have a certain tolerance against very small stimulations. However, if a relatively low threshold is crossed, they start to produce activating substances, and—at least in this *in vitro* system—the positive feedback loop is able to drive the system into an activated state. This simple model, which only aims at the first, activating phase, is not able to predict the further fate of the system: if the ECs will relax again after a longer time (we can see hints for this behavior in experiments) or if there is an external signal necessary that stops the activation of cells again.

IN VIVO MODEL

Model Equations

In the first part of the present paper we analyzed in detail the reaction of only one cell type with respect to only a few mediators. We now go into the other extreme: we consider the innate immune system as a whole and investigate the reaction of the immune system that incorporates only the most important parts of an inflammatory response. We do not aim to describe the phenomena of acquired immunity but rather at the early phase of unspecific inflammatory pathways.

This model consists of three equations, each of them representing a simplified version of a complex subsystem. The three components are (see Fig. 3): the challenge x, the inflammatory response y and the part of the immune system z that suppress the response again. The challenge triggers the proinflammatory response y (that may be represented by IL-1, endothelium and leukocytes), that fights the challenge, and—at the same time—activates the part of the immune system that suppresses an inflammatory response z (e.g. IL-10).

In more detail, we assume that the challenge is not a pathogen or alike, but e.g. a dose of IL-1 or another proinflammatory mediator (an experiment that is frequently carried out). These proinflammatory mediators vanish very soon from the system (Dinarello *et al.*, 1987). In real situations, this proinflammatory mediator has to be replaced by a pathogen or an aseptic insult, with its own dynamics. However, the density of the mediator can be

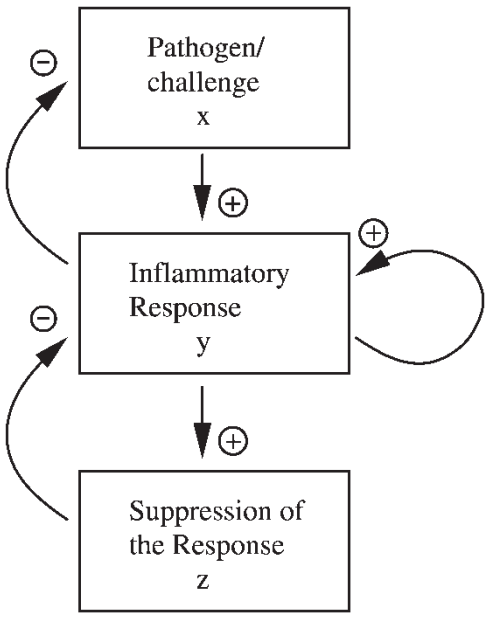

FIGURE 3 Structure of the lumped model of the immune system.

described by an exponential decay,

$$\frac{dx(t)}{dt} = -\gamma_1 x \tag{3}$$

The inflammatory response is triggered by the challenge. The density x of the proinflammatory mediator represents a challenge $\eta_1 x$ of the inflammatory response. Without the deactivating part of the immune system, this response has bistable characteristics. We have found this characteristic in the first part of the paper: If we (artificially) knock out challenge and suppression, the state of the inflammatory response y tends to zero if $y < \zeta_1$ for some $\zeta_1 > 0$. Above ζ_1 the inflammatory response tends to its maximum ζ_2. The rate η_2 determines the time scale of the inflammatory response. Hence, without the suppression of the excitation we obtain

$$\frac{dy(t)}{dt} = \eta_1 x - \eta_2 y[(\zeta_1 - y)(\zeta_2 - y)].$$

In order to formulate the deactivating effect of the variable z, we assume that $\eta_3 z + \eta_4$ is a rate that stabilizes the resting state of y. We include the constant η_4 in order to normalize the state variable z.

$$\frac{dy(t)}{dt} = \eta_1 x - \eta_2 y[(\zeta_1 - y)(\zeta_2 - y) + \eta_3 z + \eta_4]. \tag{4}$$

The dynamics of the suppressor is given by the activation of the suppression subsystem with rate δy, and a natural tendency to go into the resting state $z = 0$ with rate γ_3. Hence,

$$\frac{dz(t)}{dt} = \delta y - \gamma_3 z. \tag{5}$$

For sure, this system is only a caricature of the regulatory pathways that control the inflammatory process. Nevertheless, this model represents the current paradigm of the general structure of the innate immune system: dynamics of the challenge, the proinflammatory process and the control of the proinflammatory process by a suppressor. However, many effects are not taken into account. Not only the many details like the overwhelming variety of different and specialized cell types and mediators, but also some basic properties are neglected: the spatial structure, the suppression of IL-10 by IL-10, i.e. a negative feedback of the suppressor on itself etc. Nevertheless, this model represents the leading opinion of the medical community about the overall structure of the innate immune system, and—as such—has to be taken seriously.

Remark 4.1 (1) The density $x(t)$ decays exponentially, and we are left with a two-dimensional system. The limiting behavior of the three-dimensional system will be governed by the two-dimensional subsystem. This is ensured by the theory of asymptotically autonomous systems (Thieme, 1992).

The structure of the subsystem (4), (5) is quite similar to that of the Fitzhugh–Nagumo equations (see, e.g. Murray, 1989). The main difference is the way the inhibiting variable z enters the dynamics of y. While in the Fitzhugh–Nagumo system z enters in an purely additive manner, here z is multiplied with y, i.e. z assumes rather the role of an inhibiting rate. The Fitzhugh–Nagumo equation describe the differences of densities of ions that may change sign, while we deal here with absolute densities: positivity has to be ensured. This difference expresses itself in the different terms describing the action of the inhibitor on the reaction.

Analysis of the System

We aim at information about the transient and asymptotic behavior of the two dimensional subsystem. These results describe the behavior e.g. after a short infusion of IL-1, inducing an initial impulse to activate the immune system.

In order to reduce the number of parameters, we rescale the system. Let $z = a\tilde{z}$, $y = b\tilde{y}$, $\tau = ct$ with $c = 1/\gamma_3$, $b^2 = 1/(c\eta_3)$, and $a = (\delta b^2)/(\eta_3 \delta)$. We obtain under the condition that $x(t) \equiv 0$

$$\frac{d\tilde{y}(\tau)}{d\tau} \doteq -\tilde{y}\,[\,\tilde{y}^2 - (\zeta_1 + \zeta_2)/b\tilde{y} + \tilde{z} + (\eta_4 + \zeta_1\zeta_2)/b^2]$$

$$\frac{d\tilde{z}(\tau)}{d\tau} = \frac{\delta bc}{a}\tilde{y} - \tilde{z}$$

We define the lumped parameters

$$\mu = \frac{\zeta_1 + \zeta_2}{b} \in \mathbb{R}_+, \quad \nu = \frac{\delta bc}{a} \in \mathbb{R}_+,$$

$$\psi = (\eta_4 + \zeta_1\zeta_2)/b^2 \in \mathbb{R}.$$

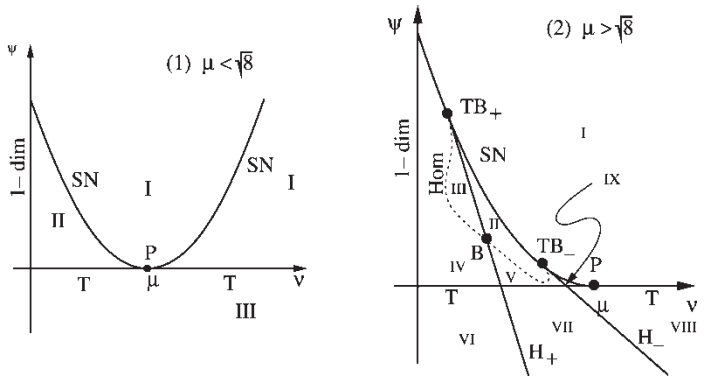

FIGURE 4 Bifurcation diagram (1) for $\mu < \sqrt{8}$ and (2) for $\mu > \sqrt{8}$. $1-$dim denotes the line, on which the system becomes essentially one-dimensional, T denotes the line of transcritical bifurcations SN denotes the line of saddle-node bifurcations and P denotes the pitchfork bifurcation. Sketches of the phase diagrams in regions I–III can be found in Fig. 5. In case (2), we have, in addition to these bifurcation points and-lines, two Bogdanov–Takens Bifurcations ($TB_{\pm}$), the corresponding Hopf lines $H_{\pm}$ and a line of homoclinic orbits (Hom, dashed line), connecting $TB_{\pm}$ and a singular (non-proper) Bautin point B. The Roman numbers denote regions of different behavior. In III, unstable periodic orbits surround (y_+^*, z_+^*), which in V and VII stable periodic orbits are located around (y_+^*, z_+^*). Sketches of the phase diagrams in regions I–X can be found in Fig. 6.

Renaming $\tilde{y}$ and $\tilde{z}$ by y and z again we are left with

$$\frac{dy(t)}{dt} = -y[\,y^2 - \mu y + z + \psi] \tag{6}$$

$$\frac{dz(t)}{dt} = \nu y - z \tag{7}$$

One may view ψ as a measure of the stability of the resting state. ν gives information about the strength of the stimulation of the suppressing control mechanism z by the proinflammatory process y. Most difficult to interpret is the parameter μ: μ controls the distance of the nontrivial equilibria. The larger μ, the more these equilibria are separated. One may take μ as a measure of the strength of the inflammatory excursion.

The details of the bifurcation analysis can be found in Appendix B. Of course, we have (like in the *in vitro* model) always a trivial equilibrium, where all cell lines are resting. For certain parameter ranges, there appear non-trivial steady states (where a certain part of cells are activated), and also periodic orbits may exist. There are two different situations to distinguish.

Case 1: $\mu < 2\sqrt{2}$

We distinguish three different cases (see Figs. 4 and 5): either there is only the trivial stationary point (s.t. this trivial stationary point is globally stable), or there are one or two additional, nonnegative and nontrivial stationary points. The parameter regions for these three cases are separated by a saddle-node (SN) and a transcritical (T) bifurcation line. These two bifurcation lines intersect in a pitchfork bifurcation. No periodic orbits appear. If two stationary points are present in the system, we find a bistable behavior: the trivial stationary point as well as one of the nontrivial stationary points are stable.

Case 2: $\mu > 2\sqrt{2}$

In this case, the behavior is more complex (see Fig. 4). The fundamental structure (no, one or two non trivial stationary points are present in the positive quadrant) is not changed. However, at the saddle-node line two Takens Bogdanov bifurcations appear (TB_+ and TB_-). They are the starting points of two straight half-lines of Hopf bifurcations (H_+ and H_-) and connected by an homoclinic line (HOM). At H_+, a Bautin point B is located, separating the part of H_+ where unstable orbits are created that are destroyed at the homoclinic line, and the part where stable periodic orbits appear. The latter vanish again in a backward Hopf bifurcation at H_-. So far, the scenario is that one expects near a co-dimension three bifurcation of the saddle-node bifurcation of two Takens–Bogdanov points. However, numerical analysis seems to hint that the homoclinic line also crosses the point B and that we have

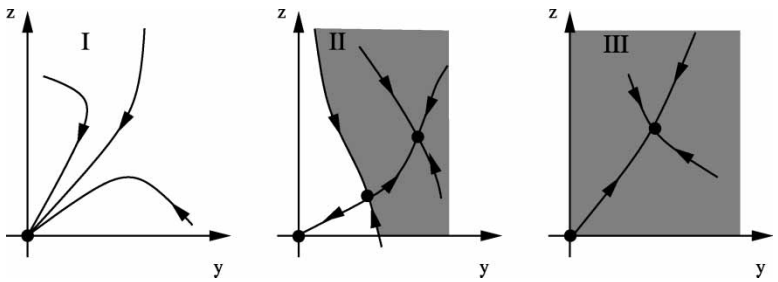

FIGURE 5 Sketch of the dynamics in different parameter regions. Parts of the phase plane that are not in the basin of attraction of the trivial solution are grey.

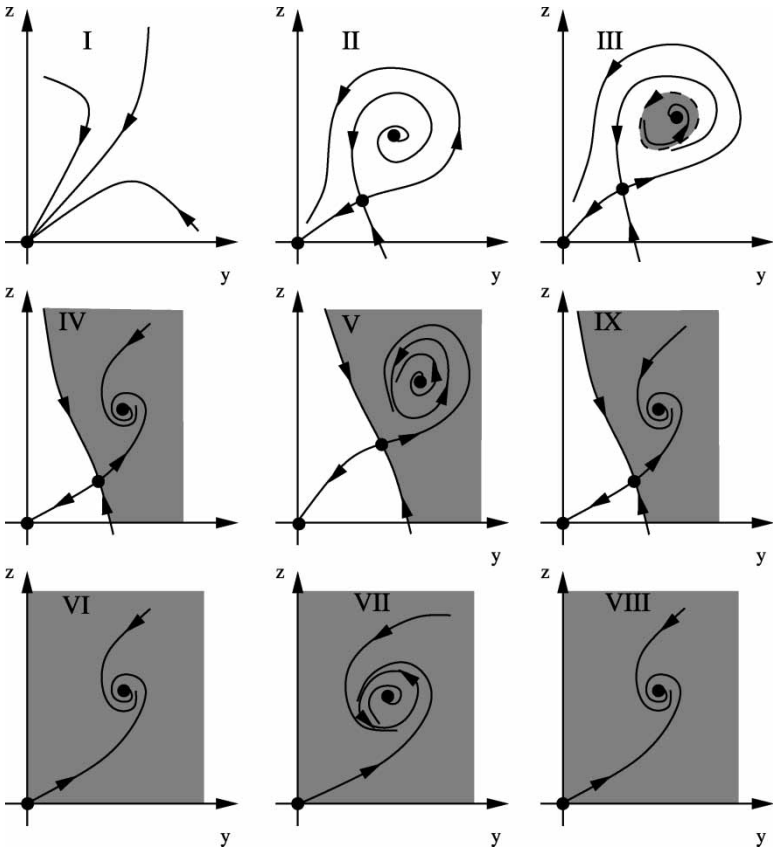

FIGURE 6 Sketch of the dynamics in different parameter regions. Parts of the phase plane that are not in the basin of attraction of the trivial solution are grey.

here a singular situation: the homoclinic loop is filled by periodic orbits (see Figs. 5–7).

In this bifurcation diagram, one may distinguish nine different regions of behavior (region I–IX). The dynamics corresponding to the different regions are shown in Fig. 6. In view of the application, one can summarize four different situations: (1) in region I the resting state is globally stable. (2) In regions II and III the resting state is still globally stable, but there is a sensitive dependence on the initial value: below a certain threshold of y, the trajectory returns more or less directly to the trivial state, while above this threshold there will be a large excursion with a large inflammatory reaction first (it is to expect that the bistable behavior in region II does not play an important role). (3) In regions IV, V and IX we find a bistable behavior: below a certain threshold for y the trajectory returns to zero; above it will approach a permanently activated state. This activated state may exhibit oscillations. (4) In regions VI, VII and XIII the resting state is not stable any more, but the system will always be in a (perhaps oscillatoric) activated state.

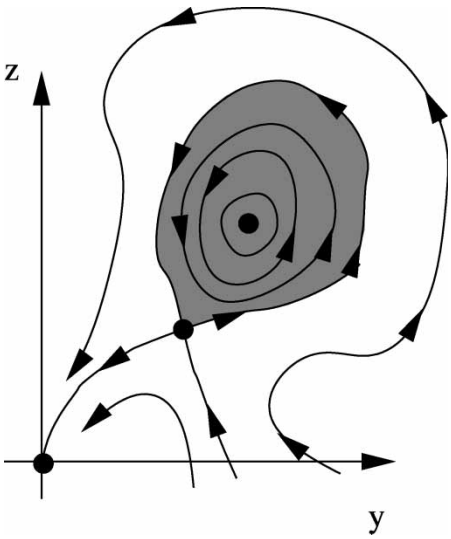

FIGURE 7 Sketch of the situation found numerically in the *B*-point: The region bounded by the homoclinic loop (shown in grey) is filled with nested periodic orbits.

Comparison with Experimental and Clinical Observations

The patterns of behavior seen at this very basic stage of modeling with respect to clinical phenomena in patients have to be interpreted cautiously. However, many experiments can be clearly explained by this model. The strength of the model is its generality—we did not specify certain mechanisms. Thus, the outcome should

be quite stable, and we expect to find the scenarios predicted by the model in reality. Of special physiological interest is the case $\mu > 2\sqrt{2}$.

1. *Regions II, III:* A small challenge is ignored, a challenge above a certain threshold leads to a large inflammatory response that eventually comes to rest again.

   This seems to be the physiological behavior. It is observed in *in-vivo* experiments like that of Dinarello *et al.* (1987). Especially, the threshold behavior is well documented in the review article (Leon, 2002, and citations there), where a small amount of IL-1 does only lead to a limited reaction (in this experiment, the read-out system is fever), while a higher dose leads to a massive strike of the immune system.
2. *Regions VI, VII, XIII:* The resting state is not stable; there may be oscillations.

   The organism is caught in a state of persistent activation of the proinflammatoric system. This phenomenon is known from a variety of clinical scenarios. In systemic disorders, like the systemic inflammatory response syndrome many patients are caught in a persistent inflammatory state that cannot be altered by therapeutic interventions. Also localized inflammatory states, which can be found, for example, in rheumatic diseases like rheumatoid arthritis, display similar features. In the case of inflammatory conditions in joints the inflammation is caught in a state of persistent activation as well, where the proinflammatory activity of IL-1 and TNF alpha is enhanced, such that the antiinflammatory reaction is not able to stabilize the resting state (Kavanaugh, 1999). In this case the resting state is only reached after therapeutic intervention.
3. *Region I:* Resting state is globally stable.

   This parameter region can be artificially reached by immunosuppressant substances. This principle is applied in clinical medicine in a variety of conditions. Chang *et al.* showed that nonsteroidal antiinflammatory drugs cut communication pathways of proinflammatory mediators like IL-11 (Chang *et al.*, 1990). A similar mechanism applies for steroids which inhibit the transcription of proinflammatory mediators. Thus steroids can drive the system back into the quiescent state, a mechanism that is clinically used in rheumatoid arthritis or asthma. Interestingly enough, attempts to treat systemic inflammatory disorders like the inflammatory response syndrome or sepsis with steroids have not been successful.
4. *Regions IV, V, IX:* Bistable behavior: the resting state is locally stable while there is also a stable inflammatory state (with large basin of attraction), with respective stable oscillations.

   Bistable behavior can be seen in inflammation of joints, where this inflammation can be controlled by treatment, but the next stress event will again lead to a locally sustained inflammation.

   According to the basic paradigm in the medical world, this picture also applies to the concept of primary multiple organ dysfunction (primary MODS) (Bone *et al.*, 1992). In primary MODS the initial injury is so severe that an overwhelming proinflammatory reaction dominates. Consequently, an early MODS develops. Consequently, it should be possible to control this inflammatory reaction and steer the system to the resting state. However, all treatment concepts developed so far with these ideas in mind did fail.

It is possible to relate most of the different parameter regions to biological and medical phenomena. However, the model predicts the possibility of stable oscillations. The period of these oscillations should be approximately that of the typical duration of the reaction on a massive stimulation by e.g. LPS or IL-1, i.e. for mice 4–6 h (Larsson *et al.*, 2000). Such oscillations are experimentally not documented. There are experimental results indicating a diurnal pattern (e.g. Petrovsky *et al.*, 1998). These patterns do not have a period in the appropriate range, and are most likely a consequence of the interaction between the immune system and the central nervous system.

Because of the stability of the model, the predicted periodic pattern should be possible to find experimentally, if the medical theory in its present form is appropriate. If we consider the bifurcation diagram, a constant, appropriate dose of antiinflammatory drugs should be able to induce oscillatoric behavior. Since there is no evidence in literature that this behavior occurs, one may argue that it is not present. It is possible that other mechanisms, that seem to play only a minor role, are more important than was assumed. Especially the mechanisms that allow an adaptation to a certain challenge (e.g. the reduction of receptors for proinflammatoric mediators on the cell surfaces of certain cell lines) may provide an explanation for the lack of oscillations. An experimental test could be the repeated challenge of an individual by IL-1 or LPS. If reactions on repetitions of a certain challenge decrease strongly, then we do have a hint for the relevance of this adaptation process. In this case, this adaptation process may run on a slow time scale. Also treatment strategies would have to take this process into account. It would be necessary to slightly change the overall model of the innate immune system.

DISCUSSION

In the first part of the paper, we modeled an experiment where endothelial cells have been challenged by IL-1. IL-6 has been measured. The model seems to meet the data quite well. However, from the model validation point of view, the experimental setup is not chosen in an optimal way (the purpose of the experiment was not

modeling and modeling validation). Better suited for our purposes is the concentration on the only partially activated system, i.e. sampling the time series between one and ten hours after activation, respectively focusing on doses below 1 ml/ml IL-1. Furthermore, in order to obtain a better insight into the system the time series of IL-1 and PGE_2 would be of interest. It seems that at least some endothelial cell lines deactivate themselves after a time span around 48 h. In order to get a better insight in the deactivating processes, a longer time series could be helpful.

The most important outcome of this model is information about the positive feedback loop of the endothelial cell/IL-1 system. This system has a bistable behavior, where the resting state is barely stable; there is only a very low tolerance against a challenge. Even relatively small amounts of pathogens are able to activate endothelial cells. These cells amplify a low initial signal via the positive feedback loop in connection with IL-1 and initiate the proinflammatory cascade. Of course, we considered an *in vitro* experiment. Especially a wash out effect of IL-1 by blood is not considered here. However, this effect may not be too strong in capillary vessels, since—especially at the walls of the vessel—the velocity of the blood is not too high. Furthermore, the reason for the sensitivity of the endothelial cells may be the prevention of the interruption of the positive feedback loop by locally washing out IL-1.

In the second part of the paper, we used the findings of the first part in order to derive a small model that only takes into account the most basic mechanisms. In the center is the bistable behavior of the proinflammatory reaction. Without a control of this reaction, a small challenge is neglected while a challenge above a certain threshold drives the system into a completely activated state. However, the immune system also includes a part that suppresses inflammatory reactions. This suppressing part is activated by the proinflammatory process.

We analyzed the possible behavior of this system in the absence of a direct challenge (representing e.g. experiments, where an animal receives an infusion of IL-1. This challenging IL-1 vanishes after at most 10 min and yields after that time an activated inflammatory network without actual challenge). We find that the resting state may be globally stable, but with a density-dependent time course. While a small challenge is almost ignored, above a certain threshold we find a large inflammatory reaction that vanishes again. This seems to be the physiologic reaction upon a pathogen. Also bistable behavior (with a possible periodic activated state) can be found. A third class of behavior is the instability of the resting state, i.e. the immune system is always in an inflammatory state, perhaps in an oscillating inflammatory state. Most cases can be found in experimental and clinical observations. Only oscillations are not well documented. Since the model predicts oscillations in certain parameter ranges, this lack of experimental results in this direction may be a hint that further effects like adaptation on challenges should be incorporated into the standard model of the innate immune system.

These patterns generally match with experiments and clinical observations. Only the predicted oscillations are not clearly observed, which may be a hint that apart from the feedback loops that are taken into account, also e.g. adaptation processes may play a crucial role. Before any clinical consequences can be drawn from this modeling approach more sophisticated models have to be developed. In view of post traumatic multiple dysfunction syndromes, a model that allows the evaluation of possible therapeutic approaches has to incorporate e.g. the principle of locality into the model. The behavior of the inflammatory system at distinct anatomical locations in the organism has to be modeled in order to identify possible targets for therapeutic interventions. The inflammatory reaction is an intriguing problem that deserves more attention of modelers. One may hope that many experiments about details of the cytokinic network provide enough information to close the gap between the two parts of the present work (that describes a very small part of the network in detail and the network as a whole in an oversimplified manner). It will be then possible to "probe" different treatment strategies *in silico* and provide a useful tool for the medical sciences.

References

Alt, W. and Lauffenburger (1985) "Transient behaviour of a chemotaxis system modelling certain types of tissue inflammation", *J. Math. Biol.* **24**, 691–722.

An, G. (2001) "Agent-based computer simulation and sirs: building a bridge between basic sciences and clinical trials", *Shock* **16**(4), 266–273.

Baue, A., Faist, E. and Fry, D. (2000) *Multiple Organ Failure* (Springer).

Bone, R., Balk, R. and Cerra, F. (1992) "Definitions for sepsis and organ failure and guidelines for the use of innovative therapies in sepsis. The ACCP/SCCM Consensus Conference Committee. American College of Chest Physicians/Society of Critical Care Medicine", *Chest*, **101**, 1644–1655.

Chang, D.M., Baptiste, P. and Schur, P.H. (1990) "The effect of antirheumatic drugs on interleukin 1 (IL-1) activity and IL-1 and IL-1 inhibitor production by human monocytes", *J. Rheumatol.* **17**, 1148–1157.

Dinarello, C. (1996) "Biological basis for interleukin-1 in disease", *Blood* **87**(6), 2095–2147.

Dinarello, C., Ikemjia, T., Warner, S., Orencole, S., Lonnemann, G., Cannon, J. and Libby, P. (1987) "Interleukin 1 induces interleukin 1. I. induction of circulating interleukin 1 in rabbits *in vivo* and in human mononuclear cells *in vitro*", *J. Immunol.* **139**(6), 1902–1910.

Dixit, V., Green, S., Sarma, V., Holzmann, L., Wolf, F., O'Rouke, K., Ward, P., Prochownik, E. and Marks, R. (1990) "Tumor necrosis factor-α induction of novel gene products in human endothelial cells including a macrophage-specific chemotaxin", *J. Biol. Chem.* **265**(5), 2973–2978.

Faist, E., Baue, A., Dittmer, H. and Heberer, G. (1983) "Multiple organ failure in polytrauma patients", *J. Trauma* **23**, 775–787.

Gilks, W., Richardson, S. and Spiegelhalter, D. (1998) *Markov Chain Monte Carlo in Practice* (Chapman and Hall).

Golubitsky, M. and Schaeffer, D. (1985) *Singularities and Groups in Bifurcation Theory* (Springer).

Guckenheimer, J. and Holmes, P. (1983) *Nonlinear Oscillations, Dynamical Systems, and Bifurcations of Vector Fields* (Springer).

Kavanaugh, A. (1999) "An overview of immunomodulatory intervention in rheumatoid athritis", *Drugs Today* **35**, 275–286.

Kuznetsov, Y.A. (1995) *Elements of Applied Bifurcation Theory* (Springer).
Larsson, R., Rockstén, D., Lilliehöök, B., Jonson, A. and Bucht, A. (2000) "Dose-dependent activation of lymphocytes in endotoxin-induces airway inflammation", *Infect. Immun.* **68**, 6962–6969.
Lauffenburger, D. (1993) *Receptors* (Oxford University Press).
Lauffenburger, D. and Kennedy, C. (1981) "Analysis of a lumped model for tissue inflammation dynamics", *Math. Biosci.* **53**, 189–221.
Leon, L.R. (2002) "Cytokine regulation of fever: studies using gene knockout mice", *J. Appl. Physiol.* **92**, 2648–2655.
Murray, J. (1989) *Mathematical Biology* (Springer).
Novak, M.A. and May, R.M. (2000) *Virus Dynamics* (Oxford Science Publications).
Perelson, A. (1987) *Theoretical Immunology* (Addison-Wesley).
Petrovsky, N., McNair, P. and Harrison, L.C. (1998) "Diurnal rhythms of pro-inflammatory cytokines: regulation by plasma cortisol and therapeutic implications", *Cytokine* **10**(4), 307–312.
Pugin, J., Schürer-Maly, C., Leturcq, D., Moriarty, A., Ulevitch, R. and Tobias, P. (1993) "Lipopolysaccharide activation of human endothelial and epithelial cells is mediated by lipopolysaccharide-binding proteins and soluble CD14", *Proc. Natl Acad. Sci. USA* **90**, 2744–2748.
Seymour, R.M. and Henderson, B. (2001) "Pro-inflammatory–anti-inflammatory cytokine dynamics mediated by cytokine-receptor dynamics in monocytes", *IMA J. Math. Appl. Med. Biol.* **18**(2), 159–192.
Shrotri, M., Peyton, J. and Cheadle, W. (2000) "Leukocyte–endothelial cell interactions: review of adhesion molecules and their role in organ injury", In: Baue, A., Faist, E. and Fry, D., eds, *Multiple Organ Failure. Pathophysiology, Prevention, and Therapy* (Springer), pp 224–243.
Sironi, M., Breviario, F., Proserpio, P., Biondi, A., Vecci, A., Van Damma, J., Dejana, E. and Mantovani, A. (1989) "IL-1 stimulates IL-6 production in endothelial cells", *J. Immunol.* **142**(2), 549–553.
Thieme, H.R. (1992) "Convergence results and a Poincare-Bendixson trichotomy for asymptotically autonomous differential equations", *J. Math. Biol.* **30**(7), 755–763.
Warner, S., Auger, K. and Libby, P. (1987) "Interleukin 1 induces interleukin 1. II. Recombinant human interleukin 1 induces interleukin 1 production by adult human vascular endothelial cells", *J. Immunol.* **139**(6), 1911–1917.

ANALYSIS OF THE *IN VITRO* MODEL

Proof (of Proposition 3.1) With the definitions $\gamma_A = \hat{\gamma}_A/\epsilon$, $A = \epsilon B$ and $r(A) = \hat{r}(A/\epsilon)$ we find the differential equations (2) for $x_0, \ldots, x_n$. The differential equation for B reads

$$\epsilon \dot{B} = -\hat{\delta}_A B + \alpha x_n.$$

$\epsilon \to 0$ yields the last equation of system (2). □

Proof: (of Proposition 3.2) For the following we rescale time by $1/\delta$ and define

$$\tilde{r}(x_n) = \frac{1}{\delta}\hat{r}(\alpha x_n/\gamma_A), \quad \tilde{\gamma}_x = \frac{1}{\delta}\gamma_x.$$

Then, system (2) reads

$$\begin{aligned}
\dot{x}_0(t) &= -\tilde{r}(x_n)\,x_0(t) + \tilde{\gamma}_x x_n(t),\\
\dot{x}_1(t) &= \tilde{r}(x_n)\,x_0(t) - x_1(t),\\
\dot{x}_i(t) &= x_{i-1}(t) - x_i(t),\\
\dot{x}_n(t) &= x_{n-1}(t) - \tilde{\gamma}_x x_n(t)
\end{aligned} \tag{8}$$

ad (1) Since $\tilde{r}(0) = 0$ the state $x_0 = 1$ and $x_i = 0$ for $i > 0$ is a stationary state. **ad (2), (3)** The Jacobian at the trivial state reads

$$J_0 = \left(\begin{array}{c|cccc} 0 & 0 & 0 & \cdots & 0 & \gamma_x - \tilde{r}'(0) \\ \hline 0 & -1 & 0 & \cdots & 0 & \tilde{r}'(0) \\ 0 & 1 & -1 & \cdots & 0 & 0 \\ 0 & 0 & 1 & \cdots & 0 & 0 \\ \vdots & \vdots & & \vdots & \vdots & \vdots \\ 0 & 0 & 0 & \cdots & -1 & 0 \\ 0 & 0 & 0 & \cdots & 1 & -\gamma_x \end{array}\right).$$

This matrix is in block-diagonal form, where the first "block" consists of the element $((J_0))_{1,1}$ and the second block is $\hat{J}_0 = ((J_0))_{2\ldots n,\,2\ldots n}$. Therefore we always find one eigenvalue zero that is caused by the trivial stationary state $(1, 0, 0\ldots, 0)^T$ together with the conservation law $\sum x_i = 1$. The eigenvalues of the larger block $\hat{J}_0$ determine the stability of the stationary state.

Case 1: $\tilde{r}'(0) = 0$: The second block $\hat{J}_0$ becomes a lower triangular matrix. The eigenvalues are -1 and $-\gamma_x$. The spectrum of the relevant part of J_0 has a negative real part, and in this case the trivial fixed point is locally stable.

Case 2: $\tilde{r}'(0) > 0$, γ_x small: The characteristic polynomial of $\hat{J}_0$ is given by

$$p(\lambda) = (\gamma_x + \lambda)(1 + \lambda)^{n-2} - \tilde{r}'(0).$$

We know that $\lim_{\lambda\to\infty} p(\lambda) = \infty$. For $\gamma_x < \tilde{r}'(0)$ we find $p(0) < 0$, and hence there is at least one positive root. Therefore the trivial state is unstable if γ_x is small.

Case 3: $\tilde{r}'(0) > 0$, γ_x large: Define $\epsilon = 1/\gamma_x$. If we divide $p(\lambda)$ by γ_x we find that $p(\lambda) = 0$ is equivalent to $\tilde{p}(\lambda) = 0$ with $\tilde{p}(\lambda) = (1 + \epsilon\lambda)(1 + \lambda)^{n-2} - \epsilon\tilde{r}'(0)$. Hence, for $\epsilon \to 0$ we have $n - 2$ eigenvalues near -1: $\lambda_1, \ldots, \lambda_{n-2} = -1 + \mathcal{O}(\epsilon)$. These eigenvalues have a negative real part (for ϵ small enough, i.e. γ_x large enough). Since the degree of p and $\tilde{p}$ is $n - 1$, there is one more eigenvalue. The coefficient of the highest order term of $\tilde{p}$ vanishes for $\epsilon = 0$. Hence there is one eigenvalue of the from $\lambda = \mathcal{O}(\epsilon^{-1})$. In order to obtain information of the sign of the real part of this eigenvalue, we define $u = 1/\lambda$ and

$$\hat{p}(u, \epsilon) = u(u + 1)^{n-2} + \epsilon((u + 1)^{n-2} - \tilde{r}'(0)u^{n-1}).$$

We find $p(\lambda) = 0$ if and only if $\hat{p}(1/\lambda, \epsilon) = 0$. Since $\hat{p}(0, 0) = 0$, $\hat{p}_u(0, 0) = 1$ and $\hat{p}_\epsilon(0, 0) = n - 2$ we conclude with the theorem about implicit functions that

$$u(\epsilon) = -(n - 2)\epsilon + \mathcal{O}(\epsilon^2).$$

Hence, $u(\epsilon)$ is negative for a small ϵ, such that all eigenvalues of $\hat{J}_0$ have negative real parts and the trivial state is locally stable if γ_x is large.

ad (4) Let $\hat{x} = (\hat{x}_1, \ldots, \hat{x}_n)$ be a stationary state. Then, $\hat{x}_1 = \ldots = \hat{x}_{n-1}$. With $z = \hat{x}_1$ we find $\hat{x}_n = z/\gamma_x$ and the condition for z

$$z = G(z) = \tilde{r}(z/\gamma_x)(1 - (n - 2 + 1/\gamma_x)z).$$

Since we are only interested in non-negative solutions, any feasible solution is located in the interval $I(\gamma_x) = [0, \gamma_x/(1 + \gamma_x(n-2))]$. Furthermore, we obtain

$$\max_{z \in I(\gamma_x)} \frac{\mathrm{d}}{\mathrm{d}z} G(z) = \max_{\tilde{z} \in [0, 1/(1+\gamma_x(n-2))]} \frac{1}{\gamma_x}$$

$$\times \frac{\mathrm{d}}{\mathrm{d}\tilde{z}} (\tilde{r}(\tilde{z})(1 - ((n-2)\gamma_x + 1)\tilde{z})) \to 0 \quad \text{for} \quad \gamma_x \to \infty.$$

Especially, $G'(z) < 1$ for $z \in I(\gamma_x)$ and γ_x sufficiently large. In this case, there is only the trivial stationary state $z = 0$.

We now show that there is a stationary point in the interval $[1 - \mathcal{O}(\gamma_x), 1]$ if $\gamma_x \to 0$. Since $G(\gamma_x/(1 + \gamma_x(n-2)) = 0$, it is enough to show that there is a positive constant c, s.t. $G(1 - c\gamma_x) > 1 - c\gamma_x$ (if γ_x is small). We find

$$\tilde{r}(1/\gamma_x - c)(1 - (n - 2 + 1/\gamma_x)(1 - c\gamma_x)) > 1 - c\gamma_x.$$

Multiplication with γ_x yields

$$\tilde{r}(1/\gamma_x - c)(1 + \mathcal{O}(\gamma_x)) > \mathcal{O}(\gamma_x).$$

Since the limit $\lim_{x \to \infty} \tilde{r}(x)$ exists and is positive, this inequality is fulfilled if γ_x is sufficiently small.

ad (5) We investigate a stationary point that approaches $(0, \ldots, 0, 1)^T$ for $\gamma_x \to 0$. Therefore we transform the system (8),

$$x_i(t) = \gamma_x y_i(t), \quad \text{for} \quad i = 0, \ldots, n-1,$$

$$x_n(t) = 1 - \gamma_x y_n(t).$$

From $\sum x_i = 1$ we obtain $y_n = \sum_{i=0}^{n-1} y_i$ and thus it is possible to eliminate y_n from the set of equations,

$$\begin{aligned}
\dot{y}_0(t) &= -\tilde{r}\left(1 - \tilde{\gamma}_x \sum_{i=0}^{n-1} y_i\right) y_0(t) + 1 - \tilde{\gamma}_x \sum_{i=0}^{n-1} y_i, \\
\dot{y}_1(t) &= \tilde{r}\left(1 - \tilde{\gamma}_x \sum_{i=0}^{n-1} y_i\right) y_0(t) - y_1(t), \\
\dot{y}_i(t) &= y_{i-1}(t) - y_i(t).
\end{aligned} \tag{9}$$

Hence, the nontrivial fixed point $y^*(\tilde{\gamma}_x)$ in this transformed system reads for $\tilde{\gamma}_x \to 0$

$$\lim_{\tilde{\gamma}_x \to 0} y^*(\tilde{\gamma}_x) = (y_0, \ldots, y_{n-1})^T = (\tilde{r}(1)^{-1}, 1, \ldots, 1)^T.$$

Since $y^*(\tilde{\gamma}_x) = y^*(0) + \mathcal{O}(\tilde{\gamma}_x)$, we find the Jacobian at this fixed point

$$J^* = J_0^* + \tilde{\gamma}_x J_1^*(\tilde{\gamma}_x)$$

where $J_1^*(\tilde{\gamma}_x)$ is a bounded matrix valued function that depends continuously on $\tilde{\gamma}_x$ and

$$J_0^* = \begin{pmatrix}
-\tilde{r}(1) & 0 & \cdots & 0 & 0 \\
\tilde{r}(1) & -1 & \cdots & 0 & 0 \\
0 & 1 & \cdots & 0 & 0 \\
\vdots & \vdots & & \vdots & \vdots \\
0 & 0 & \cdots & -1 & 0 \\
0 & 0 & \cdots & 1 & -1
\end{pmatrix}.$$

The spectrum of J_0^* consists of $\{-\tilde{r}(1), -1\}$. Since J^* is the sum of J_0^* and the small perturbation $\tilde{\gamma}_x J_1^*(\tilde{\gamma}_x)$, the state y^* is stable provided that γ_x is small enough. □

ANALYSIS OF THE *IN VIVO* MODEL

Invariant Positive Region

PROPOSITION 2.1: In $\mathbb{R}_+^2$, a positively invariant, absorbing region exists.

Proof: Consider $G = \{(y, z) \,|\, x, y \in \mathbb{R}_+, \quad y + z \le C\}$. The boundary of this region consists of parts of the two axis (which are invariant under the flow) and the line $y + z = C$. We show that the vector field points inward at this line, provided that C is chosen large enough. The inner normal at this line is $\mathbf{n} = (-1, -1)^T$. Let F be the vector field (6), (7). Then,

$$\mathbf{n}^T F(y, z) = y(y^2 - \mu y + z + \psi) - \nu y + z.$$

Since $z = C - y$ at the line, we find

$$\mathbf{n}^T F(y, z) = y(y^2 - (\mu + 1)y + C - 1 + (\psi - \nu)) + C.$$

If we choose C large enough, there is no real root of $y^2 - (\mu + 1)y + C - 1 + (\psi - \nu)$. Hence, the whole expression is always positive, and the flow points inward at this part of the boundary of G. Hence, G is invariant. Since this is true for all C large enough, we find that G is even absorbing in $\mathbb{R}^2$. □

Stationary Points

PROPOSITION 2.2: There is always the trivial stationary point $(y, z) = (0, 0)$. If $(\mu - \nu)^2 \ge 4\psi$, then there are two more stationary points (for $(\mu - \nu)^2 = 4\psi$ counted with multiplicity),

$$\left(y_\pm^*, z_\pm^*\right) = \left(\frac{1}{2}\left[-(\nu - \mu) \pm \sqrt{(\nu - \mu)^2 - 4\psi}\right],\right.$$

$$\left. \nu \frac{1}{2}\left[-(\nu - \mu) \pm \sqrt{(\nu - \mu)^2 - 4\psi}\right]\right)$$

Proof: From $\dot{z} = 0$ we conclude $z = \nu y$, and thus $y[y^2 - \mu y + \nu y + \psi] = 0$. Thus, either $y = 0$ (and therefore also $z = 0$), or

$$y^2 + (\nu - \mu)y + \psi = 0. \tag{10}$$

The solutions of the latter quadratic polynomial yield to the nontrivial stationary points. □

Local Bifurcations of Codimension One

Transcritical Bifurcation

PROPOSITION 2.3: The trivial stationary point undergoes a transcritical bifurcation for $\psi = 0$, if $\psi \neq \mu$.

Proof: The trivial stationary point does exist for all parameter values. The Jacobian at the trivial stationary point reads

$$J|_{(0,0)} = \begin{pmatrix} -\psi & 0 \\ \nu & -1 \end{pmatrix},$$

i.e. the eigenvalues are $-\psi$ and -1. This point is a stable node for $\psi > 0$ while it is a saddle for $\psi < 0$. If ψ goes from positive to negative values and $\mu \neq \nu$, then (y_-^*, z_-^*) crosses (0,0). □

Saddle-Node Bifurcation

PROPOSITION 2.4: For $4\psi = (\mu - \nu)^2$ and $\nu \neq \mu$ a saddle-node bifurcation occurs. At this bifurcation, the stationary points are both positive for $\nu < \mu$ and negative for $\mu > \nu$.

Proof: This proposition follows directly from the explicit representation of the stationary points $(y_\pm^*, z_\pm^*)$. □

Hopf Bifurcation

PROPOSITION 2.5: If $\mu > \sqrt{8}$, there are two lines of Hopf points:

$$H_+: \quad 1 - 2\psi = \frac{1}{4}\left(\mu + \sqrt{\mu^2 - 8}\right)(2\nu - \mu)$$

$$\text{for} \quad \nu > \frac{1}{2}\left(\mu - \sqrt{\mu^2 - 8}\right),$$

$$H_-: \quad 1 - 2\psi = \frac{1}{4}\left(\mu - \sqrt{\mu^2 - 8}\right)(2\nu - \mu)$$

$$\text{for} \quad \nu > \frac{1}{2}\left(\mu + \sqrt{\mu^2 - 8}\right).$$

Proof: Since the trivial stationary point always has real eigenvalues, the only stationary points that are able to undergo a Hopf bifurcation are $(y_\pm^*, z_\pm^*)$. The Jacobian at these points reads

$$J|_{(y^*, z^*)} = \begin{pmatrix} -y^*(2y^* - \mu) & -y^* \\ \nu & -1 \end{pmatrix},$$

where (y^*, z^*) denotes either of the points $(y_\pm^*, z_\pm^*)$. The trace of the Jacobian must vanish for a Hopf bifurcation to occur. Thus, necessarily,

$$y^*(2y^* - \mu) + 1 = 0 \tag{11}$$

on the Hopf line. We use Eq. (10) in order to eliminate the quadratic term, and obtain $(2\nu - \mu)y^* + 2\psi - 1 = 0$. Thus,

$$y^* = \frac{1 - 2\psi}{2\nu - \mu}.$$

If we combine this result with the equation (10), we find

$$\begin{aligned} 0 &= \left(\frac{1 - 2\psi}{2\nu - \mu}\right)^2 + (\nu - \mu)\left(\frac{1 - 2\psi}{2\nu - \mu}\right) + \psi \\ &= \left(\frac{1 - 2\psi}{2\nu - \mu}\right)^2 + \frac{1}{2}(2\nu - \mu)\left(\frac{1 - 2\psi}{2\nu - \mu}\right) \\ &\quad - \frac{1}{2}\mu\left(\frac{1 - 2\psi}{2\nu - \mu}\right) + \psi \\ &= \left(\frac{1 - 2\psi}{2\nu - \mu}\right)^2 - \frac{1}{2}\mu\left(\frac{1 - 2\psi}{2\nu - \mu}\right) + \frac{1}{2}. \end{aligned}$$

Therefore

$$\frac{1 - 2\psi}{2\nu - \mu} = \frac{1}{4}\left(\mu \pm \sqrt{\mu^2 - 8}\right),$$

i.e. all Hopf points are located on the lines $H_\pm$ (by now without the restriction on ν).

On these two lines $\operatorname{tr}(J|_{y^*, z^*}) = 0$, i.e. one of two necessary conditions for a Hopf bifurcation to occur is satisfied. The second necessary condition is $\det(J|_{y^*, z^*}) > 0$,

$$y^*(2y^* - \mu) + \nu y^* > 0.$$

From $\operatorname{tr}(J|_{y^*, z^*}) = 0$ we conclude that

$$y^*(2y^* - \mu) = -1, \quad y^* = \frac{1}{4}\left(\mu \pm \sqrt{\mu^2 - 8}\right)$$

and hence $\det(J|_{y^*, z^*}) = \nu y^* - 1 > 0$, i.e.

$$\nu > \frac{1}{y^*} = \frac{4}{\mu \pm \sqrt{\mu^2 - 8}} = \frac{1}{2}\left(\mu \mp \sqrt{\mu^2 - 8}\right).$$

□

PROPOSITION 2.6: All points on H_- correspond to proper Hopf bifurcations, while at all points on H_+ except

of $(\nu, \psi) = (\mu/2,\ 1/2)$ proper Hopf bifurcation takes place.

Proof: Two conditions have to be checked: first, that the eigenvalues cross the imaginary axes properly, second that the third-order term of the radial component of the dynamical system transformed in polar coordinates does not vanish.

Eigenvalues:

Close to the Hopf line, the eigenvalues are not real, i.e. $\Re(\lambda_\pm) = -\mathrm{tr}\,(J|_{y^*,z^*})$. Hence,

$$\Re(\lambda_\pm) = -\frac{1}{2}(1 + y^*(2y^* - \mu)) \Rightarrow \frac{\partial}{\partial \nu}\Re(\lambda_\pm)|_{H_\pm} = -2\left(\frac{\partial}{\partial \nu}y^*\right)\left[y^* - \frac{\mu}{4}\right]\Big|_{H_\pm}.$$

Differentiating Eq. (10) with respect to ν yields

$$\frac{\partial}{\partial \nu}y^* = \frac{-y^*}{2y^* - \mu + \nu}.$$

On the Hopf line, y^* is explicitly known from equation (11), $y^* = \frac{1}{2}(\mu \pm \sqrt{\mu^2 - 8})$. Hence,

$$\frac{\partial}{\partial \nu}\Re(\lambda_\pm) = -\frac{1}{2}\sqrt{\mu^2 - 8}\,\frac{\mu \pm \sqrt{\mu^2 - 8}}{2y^* - \mu + \nu}.$$

Since $\mu \pm \sqrt{\mu^2 - 8} > 0$, the only change of sign is possible for $2y^* - \mu + \nu = 0$. From $\nu = -(2y^* - \mu)$ and $\mathrm{tr}\,(J|_{y^*,z^*}) = 0$ we conclude $1 + \nu y^* = 0$, i.e. $\det(J|_{y^*,z^*}) = 0$, a contradiction to $\det(J|_{y^*,z^*}) > 0$ on $H_\pm$. Therefore, $(\partial/\partial\nu)\Re(\lambda_\pm)$ does not change its sign on $H_\pm$.

Third-order term of the radial component:

Let $\omega = \sqrt{\det(J|_{y^*,z^*})} = \sqrt{\nu y^* - 1}$ be the angular frequency of the system at the Hopf line, and $\lambda_\pm = \pm i\omega$ the eigenvalues. The complex eigenvector reads

$$X := \begin{pmatrix} 1 \\ \nu \end{pmatrix} + \mathrm{i}\omega \begin{pmatrix} 1 \\ 0 \end{pmatrix}.$$

We define new variables u, v by

$$\begin{pmatrix} y - y^* \\ z - z^* \end{pmatrix} = \Re(X)\,v + \Im(X)\,u = \begin{pmatrix} v + \omega u \\ \nu v \end{pmatrix}$$

and obtain the transformed system (note that the transformation is only valid on the Hopf lines, since the conditions $H_\pm$ are used)

$$\dot{u} = -\omega v + f(u, v)$$

$$\dot{v} = \omega u + g(u, v)$$

with

$$f(u,v) = -\frac{1}{\omega}(\omega u + v)[(\omega u + v)^2 + (3y^* - \mu)(\omega u + v) + \nu v],$$

$$g(u,v) = 0.$$

For a proper Hopf bifurcation to occur, the coefficient a defined by

$$a = \frac{1}{16}[f_{uuu} + f_{uvv} + g_{vvu} + g_{vvv}] + \frac{1}{16\omega}[f_{uv}(f_{uu} + f_{vv}) - g_{uv}(g_{uu} + g_{vv}) - f_{uu}g_{vv} + f_{vv}g_{uu}]$$

must not vanish (Guckenheimer and Holmes, 1983, Chapter 3.4). We obtain

$$a = -\frac{3}{8}(1 + \omega^2) + \frac{1}{8\omega^2}(6y^* - 2\mu + \nu)[(1 + \omega^2)(3y^* - \mu) + \nu].$$

The relation $\omega^2 = \nu y^* - 1$ leads to

$$a = -\frac{3}{8}\nu y^* + \frac{1}{8(\nu y^* - 1)}(6y^* - 2\mu + \nu)[\nu y^*(3y^* - \mu) + \nu].$$

With $y^*(2y^* - \mu) + 1 = 0$ we find

$$a = \frac{\nu y^*}{8(\nu y^* - 1)}[y^*(2y^* - 2\nu) + 1].$$

Since $\nu y^* - 1 = \det(J|_{y^*,z^*}) > 0$ and $y^* > 0$, it follows that $a = 0$ is equivalent with $y^*(2y^* - 2\nu) + 1 = 0$. Since the trace vanishes on the Hopf line, we have

$$\mathrm{tr}(J|_{y^*,z^*}) = y^*(2y^* - \mu) + 1 = 0,$$

and thus

$$\nu = \frac{\mu}{2} \Rightarrow \psi = \frac{1}{2}.$$

This point is located on H_+. Hence, H_- is a line of proper Hopf bifurcation, while on H_+ at $(\nu,\psi) = (\mu/2, 1/2)$ the third order term of the radial component changes its sign. □

Remark 2.7: **(a)** The change of the sign of a on H_+ is a hint that a Bautin bifurcation happens at $(\nu, \psi) = (\mu/2, 1/2)$. Therefore we call this point "B". However, we will see later that not a local bifurcation of higher codimension but a global bifurcation occurs here.

(b) Crossing the line H_- from left to right (i.e. increasing in ν), the eigenvalues of the stationary point that undergoes the Hopf bifurcation are changing from negative to positive. Increasing ν further and crossing H_-, the eigenvalues become positive again. Since the coefficient a is negative on H_+ between TB_+ (see below) and B, unstable periodic orbits appear on the left hand side of H_+. a becomes positive on the remaining part of H_+ and on H_+, leading to the emergence of stable

orbits on the right hand side of H_+ and for $\nu > \mu/2$, and on the left hand side of H_-.

Local Bifurcations of Codimension Two

Pitchfork Bifurcation

PROPOSITION 2.8: At $(\nu, \psi) = (\mu, 0)$ a pitchfork bifurcation takes place.

Proof: The proof follows at once from the structure of the stationary points. □

Remark 2.9: In Guckenheimer and Holmes (1983) the pitchfork bifurcation is called a bifurcation of codimension one. This is only true, if some symmetry conditions for the vector field hold true. Without symmetry, like in our case, two parameters are needed to unfold the pitchfork bifurcation (see also Golubitsky and Schaeffer, 1985).

Takens–Bogdanov Bifurcation

PROPOSITION 2.10: Let $TB_\pm$ denote the points

$$TB_+ : (\nu, \psi) = \left(\frac{1}{2}\left(\mu - \sqrt{\mu^2 - 8}\right),\ \frac{1}{16}\left(\mu + \sqrt{\mu^2 - 8}\right)^2\right),$$

$$TB_- : (\nu, \psi) = \left(\frac{1}{2}\left(\mu + \sqrt{\mu^2 - 8}\right),\ \frac{1}{16}\left(\mu - \sqrt{\mu^2 - 8}\right)^2\right).$$

in the parameter plane. Then, for $\mu > \sqrt{8}$, at $TB_\pm$ proper Takens–Bogdanov bifurcations are located.

Proof: In the first step we slightly transform our dynamical system into a more handsome shape. For this transformed system we apply the theorem about Takens–Bogdanov bifurcations (Kuznetsov, 1995, p. 278).

Step 1: Transformation. We shift the nontrivial stationary point (for the parameter values of $TB_\pm$) into zero and rewrite the system as a nonlinear oscillator. Let

$$z = w_1 + 1, \quad y = (w_1 + w_2 + 1)/\nu \quad \Leftrightarrow \quad w_1 = z - 1,$$

$$w_2 = \nu y - z$$

then

$$\dot{w}_1 = w_2 \tag{12}$$

$$\dot{w}_2 = -\frac{(w_1 + w_2 + 1)^3}{\nu^2} + \frac{\mu(w_1 + w_2 + 1)^2}{\nu} - (w_1 + w_2 + 1)(w_1 + 1 - \psi) - w_2. \tag{13}$$

We can write this system as

$$\dot{w}_1 = \sum_{i,j} a_{ij} w_1^i w_2^j, \quad \dot{w}_2 = \sum_{i,j} b_{ij} w_1^i w_2^j,$$

with $a_{01} = 1$ and $a_{i,j} = 0$ else, and

$$b_{00} = -\frac{1 + \nu(\nu - \mu) + \nu^2\psi}{\nu^2}$$

$$b_{01} = b_{10} = -\frac{3 + 2\nu(\nu - \mu) + \nu^2\psi}{\nu^2}$$

$$b_{20} = -\frac{3 + \nu(\nu - \mu)}{\nu^2}$$

$$b_{11} = -\frac{6 + \nu(\nu - 2\mu)}{\nu^2} = b_{20} + b_{02}$$

$$b_{02} = -\frac{3 - \nu\mu}{\nu^2}$$

Since we find $\nu(\nu - \mu) = -2$ and $\psi\nu^2 = 1$ in the Takens–Bogdanov points, it is $b_{00}|_{TB_\pm} = b_{10}|_{TB_\pm} = b_{01}|_{TB_\pm} = 0$.

Step 2: Generic conditions for a Takens–Bogdanov bifurcation

Condition 1: Form of the Jacobian

For $TB_\pm$, the Jacobian of $w = (w_1, w_2) = (0, 0)$ reads

$$A = \begin{pmatrix} 0 & 1 \\ 0 & 0 \end{pmatrix}$$

i.e. assumes the appropriate form for a Takens–Bogdanov bifurcation.

Condition 2: Nondegenerated higher-order terms

The appropriate higher-order terms of the normal form must not vanish in order to guarantee the codimension to be exactly two. Indeed, we find at the $TB_\pm$ − point

$$a_{20} + b_{11}|_{TB_\pm} = -\left.\frac{6 + \nu(\nu - 2\mu)}{\nu^2}\right|_{TB_\pm} = -\left.\frac{8 + 2(\mu \mp \sqrt{\mu^2 - 8})\mu)}{(\mu \mp \sqrt{\mu^2 - 8})^2}\right|_{TB_\pm} \neq 0$$

and

$$b_{20}|_{TB_\pm} = -\left.\frac{3 + \nu(\nu - \mu)}{\nu^2}\right|_{TB_\pm} = -\left.\frac{1}{\nu^2}\right|_{TB_\pm} \neq 0$$

Condition 3: Transversally of the parameter space

The last condition determines if a full unfolding is possible, checking first order conditions for transversality. If $g(w; \mu, \psi)$ denotes the r.h.s. of Eqs. (12), (13), then the map

$$(w_1, w_2, \mu, \psi) \mapsto \left(g(w_1, w_2, \mu, \psi), \mathrm{tr}\left(\frac{\mathrm{d}}{\mathrm{d}w} g\right), \det\left(\frac{\mathrm{d}}{\mathrm{d}w}\mathrm{g}\right)\right)$$

should be non-singular at $w = (w_1, w_2) = 0$ and $TB_\pm$. Since

$$\frac{\mathrm{d}}{\mathrm{d}w} g = \begin{pmatrix} 0 & 1 \\ b_{10} + b_{11}w_2 + b_{20}w_1 & b_{01} + b_{11}w_1 + b_{02}w_2 \end{pmatrix} + \text{higher-order terms}$$

we find

$$\mathrm{tr}\left(\frac{\mathrm{d}}{\mathrm{d}w}\mathrm{g}\right) = b_{01} + b_{11}w_1 + b_{02}w_2,$$

$$\det\left(\frac{\mathrm{d}}{\mathrm{d}w}\mathrm{g}\right) = b_{10} + b_{11}w_2 + b_{20}w_1$$

and the Jacobian of this map at the Takens–Bogdanov bifurcation

$$J = \begin{pmatrix} 0 & 1 & 0 & 0 \\ 0 & 0 & 1/\nu & -1 \\ b_{11} & b_{02} & 2/\nu & -1 \\ -b_{20} & b_{11} & -2/\nu & 1 \end{pmatrix}.$$

The determinant of this expression reads (note that we use the parameters of the Takens–Bogdanov points $TB_\pm$)

$$\det(J) = -\frac{1}{\nu}(b_{11} - b_{20}) = -\frac{1}{\nu}b_{02} = -\frac{1}{\nu^3} \neq 0$$

Therefore all conditions for Takens–Bogdanov bifurcations are satisfied. □

Remark 2.11: At the TB-points $b_{11} = 4 - \mu\nu$, the sign of

$$s = \mathrm{sign}\,(b_{20}(a_{20} + b_{11})) = \mathrm{sign}\left(\frac{8 - \mu(\mu \mp \sqrt{\mu^2 - 8})}{2\nu^4}\right)$$

is positive for TB_+ and negative for TB_-, indicating that the homoclinic orbit and the periodic orbits are unstable near TB_+ and stable near TB_-.

Global Bifurcations

One-Dimensional Singularity

PROPOSITION 2.12: For $\nu = 0$, all limit sets are included in $\{z = 0\}$, i.e. we have an essentially one-dimensional system.

Proof: The proof is immediately clear because in this case $\dot{z} = -z$, i.e. z vanishes asymptotically. □

B-Point: Singular Bautin Bifurcation and Homoclinic Line

THEOREM 2.13: The Takens–Bogdanov points $TB_\pm$ are connected by a line of homoclinic orbits. This line crosses the line H_+. Furthermore, somewhere on this line the homoclinic orbits change their stability from unstable (near TB_+) to stable (near TB_-).

Proof: The proof is primarily based on topological arguments.

Step 1: Heteroclinic connection of $y^*_\pm$ near the SN-line.

The SN-line can be split into three parts, part SN_a left of TB_+, the part SN_b between TB_+ and TB_- and the part SN_c between TB_- and P. One eigenvalue is always zero on this line, the other eigenvalue changes sign at $TB_\pm$. Since this second eigenvalue is negative in P (here, $y_\pm$ and the trivial stationary point coincides, and the trivial stationary point always has one negative eigenvalue), on SN_a and SN_c, the non-zero eigenvalue is negative, and on SN_b it is positive.

Now consider the situation very close to SN_b. We find one unstable node and one saddle. The following argument shows that y^*_- is the saddle and y^*_+ is the node: since in the interior of the parameter region bounded by SN_b, H_+, H_- and T, no local bifurcation takes place, the saddle stays a saddle and eventually undergoes the transcritical bifurcation with the trivial stationary point. Hence, y^*_- is the saddle while y^*_+ is the unstable node. y^*_- is connected via its unstable manifold with y^*_+. Similar arguments show that y^*_- is connected via the stable manifold with y^*_+ near SN_a and SN_c.

Step 2: Heteroclinic connection of $y^*_\pm$ near the 1-dim and T-line.

Since the trivial stationary point has one stable manifold (the z-axis) and one weakly unstable manifold at the line T, the unstable manifold of $y-$ (that coincides with the trivial stationary point at T) is connected with y^*_- or a periodic orbit surrounding y^*_+. At the line 1-dim, the unstable manifold of y^*_- is always connected with y^*_+.

Step 3: Detecting the homoclinic connection.

Let Ω be the set of parameter values (ν,ψ) s.t. y^*_- is connected via its stable manifold to y^*_+ (or a periodic orbit surrounding y^*_+). Due to the results of Steps 1 and 2, the set Ω cannot touch SN_a, SN_c, 1-dim or T. Therefore it is a bounded set. Furthermore, again because of Step 1, we have $SN_b \subset \partial\Omega$. On the other part of the boundary of Ω, the homoclinic connection of y^*_- and y^*_+ changes. In Ω, the stable manifold of y^*_- connects with y^*_+ (or a surrounding periodic orbit), while outside the unstable manifold of y^*_- connects to y^*_+ (respective to a surrounding periodic orbit). This change in connecting manifold can happen only via a homoclinic connection.

Step 4: Properties of the homoclinic line.

$\partial\Omega$ consists of parts of the line SN respectively of a line of homoclinic loops. To be more precise, $SN_b \subset \partial\Omega$. Since Ω is open and the points $TB_\pm$ are located at the endpoints of SN_b, there is a line of homoclinic loops that connects TB_+ and TB_-. Since we know from the normal form of TB_+, that the homoclinic line starts

left of H_+, and ends at TB_- (i.e. on the r.h.s. of H_+), it crosses H_+. Furthermore, from Remark (2.11) we know that the homoclinic line is stable near TB_- and unstable near TB_+. Hence, the homoclinic orbit changes its stability. □

Remark 2.14: Numerical simulations show that in the point B, there is no Bautin bifurcation, but nested periodic orbits bounded by the homoclinic loop (see Fig. 7). This implies that in point B a Bautin bifurcation does not take place, but the stable and unstable lines of periodic orbits with a given frequency merge in a neutral stable periodic orbit. Also, at point B, the homoclinic loops change their stability.

It is to be expected that in a system with nonlinearities of a higher order this non-generic behavior is destroyed, and one will find a proper Bautin point. The change in stability of the lines with periodic orbits of a given frequency respectively, the line of homoclinic orbits will not coincide in one parameter point, but will occur via saddle-node bifurcations of periodic orbits.